Journal of Neuroscience Methods 211 (2012) 168–178

Contents lists available at SciVerse ScienceDirect

Journal of Neuroscience Methods

journal homepage: www.elsevier.com/locate/jneumeth

Computational Neuroscience

A novel automated spike sorting algorithm with adaptable feature extraction

Robert Bestel*, Andreas W. Daus, Christiane Thielemann

BioMEMS Lab, University of Applied Sciences Aschaffenburg, 63743 Aschaffenburg, Germany

HIGHLIGHTS

- New feature extraction approach based on review of common spike sorting methods.
- Variable feature derivation by evaluating the feature's probability distribution.
- Validation of the algorithm with neuronal monolayer and 3D spheroid signal data.
- Comparison of the results with common feature extraction techniques.

ARTICLE INFO

Article history:
Received 8 May 2012
Received in revised form 13 August 2012
Accepted 15 August 2012

Keywords:
Spike sorting
Microelectrode array
Neuron
Action potential
Biosensor

ABSTRACT

To study the electrophysiological properties of neuronal networks, in vitro studies based on microelectrode arrays have become a viable tool for analysis. Although in constant progress, a challenging task still remains in this area: the development of an efficient spike sorting algorithm that allows an accurate signal analysis at the single-cell level. Most sorting algorithms currently available only extract a specific feature type, such as the principal components or Wavelet coefficients of the measured spike signals in order to separate different spike shapes generated by different neurons. However, due to the great variety in the obtained spike shapes, the derivation of an optimal feature set is still a very complex issue that current algorithms struggle with. To address this problem, we propose a novel algorithm that (i) extracts a variety of geometric, Wavelet and principal component-based features and (ii) automatically derives a feature subset, most suitable for sorting an individual set of spike signals. Thus, there is a new approach that evaluates the probability distribution of the obtained spike features and consequently determines the candidates most suitable for the actual spike sorting. These candidates can be formed into an individually adjusted set of spike features, allowing a separation of the various shapes present in the obtained neuronal signal by a subsequent expectation maximisation clustering algorithm. Test results with simulated data files and data obtained from chick embryonic neurons cultured on microelectrode arrays showed an excellent classification result, indicating the superior performance of the described algorithm approach.

1. Introduction

The most basic goal of neuroscience is undoubtedly to understand the processes of the human brain, not only to comprehend the thought process itself, but also to find methods that treat neurological diseases such as epilepsy, depression and Alzheimer's disease. One way to study the behaviour of neuronal networks is to monitor electric signals generated by various neurons in such a network. In vitro experiments enable the analysis of cell–cell interactions in controlled laboratory conditions and further offer improved research opportunities because of a reduced network complexity, as well as better accessibility. The standard technique to derive neuronal signals is the patch-clamp method (Sakmann and Neher, 2009). In recent years, however, the usage of microelectrode arrays (MEAs) has become increasingly popular, as this technique allows non-invasive and label-free recordings from multiple positions in the neuronal network (Thomas et al., 1972).

However, fundamental network analysis still faces certain difficulties, since it cannot be guaranteed that the recorded electrode signal originates only from one single cell rather than from multiple neurons in the proximity of that specific electrode. Due to this uncertainty, special methods are required to separate different cell signals within the measured electrode signal. One possible approach takes into account the fact that the derived shape of the signal changes with respect to the position of the neuron and the corresponding electrode (see Fig. 1).

However, none of the proposed spike sorting methods can be broadly established, mainly due to accuracy and performance issues. In the following report, we present an overview of spike

* Corresponding author at: Würzburger Straße 45, D-63743 Aschaffenburg, Germany. Tel.: +49 6022 81 3612; fax: +49 6022 81 3611.
E-mail address: robert.bestel@h-ab.de (R. Bestel).

0165-0270
http://dx.doi.org/10.1016/j.jneumeth.2012.08.015

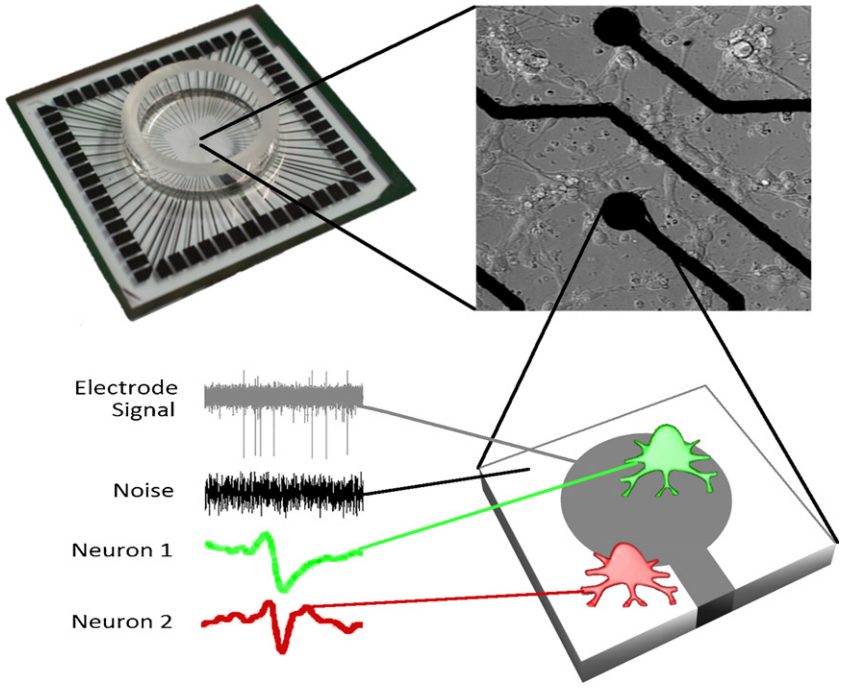

Fig. 1. Schematic of the signal components that can participate in the generation of a measured electrode signal. The signal can contain spikes generated by different neurons. The shapes of these neural spikes should vary due to different coupling qualities between the individual neuron and the electrode. In addition, noise, originating from various sources, is usually picked up by the respective electrode.

sorting algorithms already developed in this area. We also present a new approach to the spike sorting problem, focussing on possible features that are used to describe the different shape patterns of neuronal spikes. Instead of limiting the pool of possible features to a certain type, such as principal components or Wavelet-based features, the proposed algorithm calculates a variety of spike parameters. With a newly developed evaluation method, based on expectation maximisation (EM) approximation, the algorithm selects features that are the most suitable for the spike sorting of a particular dataset.

2. State of the art

An analysis of the current literature on neuronal pattern recognition reveals a wide variety of spike sorting approaches (see Table 1). Usually, most spike sorting algorithms can be divided into two major steps: feature extraction followed by classification or clustering. In addition, Table 1 also includes information about the used spike detection technique, as this pre-processing step can also influence the result of the spike sorting significantly. Many different approaches have already been tested and introduced in order to address the problem at hand.

In terms of spike detection, the most common methods use simple thresholding techniques to extract the actual spike signals from the noisy measurement data. More elaborated algorithms further add specific signal transformations, e.g. using the nonlinear or Teager energy operator (NEO or TEO) (Kim and Kim, 2000; Choi et al., 2006) to the thresholding process in order to decrease the influence of noise or low frequency signal artefacts. Another approach presented by Hulata et al. (2002) uses Wavelet-based decomposition to discriminate actual spike shapes from noise. Such extended detection methods usually yield a more precise detection result, which facilitates the actual sorting process, but at the expense of a higher computational complexity.

The most common method of feature extraction and reduction is still the principal component analysis (PCA) (Wood et al., 2004; Wang et al., 2006; Biffi et al., 2008). However, Wavelet- or Wavelet packet-based features have also become quite popular as the resulting coefficients are also capable of describing the differences of various spike signals (Oweiss and Anderson, 2002; Hulata et al., 2002; Quiroga et al., 2004). A drawback of this complex method is the necessity of an additional selection step to identify the coefficients that most precisely discriminate between the various spike shapes. In some cases, geometric features are also obtained from the measured spike events (Fee et al., 1996; Vogelstein et al., 2004) as an alternative or, more commonly, a complement to standard PCA features. The variety of the used spike sorting features indicates that no optimal feature set has yet been established. This might be due to the fact that it is questionable whether a fixed set of features exists that can generally guarantee a suitable spike shape representation.

While an analysis of common spike sorting features already shows certain diversity, this is even more apparent in the area of possible classification algorithms. Many different pattern recognition approaches, ranging from simple clustering techniques such as *k-means* (Hulata et al., 2002; Sato et al., 2007), more elaborate expectation maximisation (Kim and Kim, 2003; Wood et al., 2004) and superparamagnetic clustering methods (Quiroga et al., 2004), to trainable classification algorithms such as neural networks (Kim and Kim, 2000) and support vector machines (SVMs) (Vogelstein et al., 2004), have already been tested for neural spike sorting. However, none of these approaches has been able to provide generally optimal results to be widely established. Whereas trainable algorithms certainly provide a greater potential, their performance still seems to suffer due to a lack of fundamental training data. Unlike in other areas, for example voice recognition or person identification, in which basic training databases already exist, such datasets have not been established for neural patterns, thereby limiting actual algorithm training.

In addition, many spike sorting algorithms also include a final template matching step to further refine the classification result (Zhang et al., 2004; Wang et al., 2006; Sato et al.,

Table 1
Overview of the published spike sorting algorithms.

Author/year	Detection	Features	Classification
Hulata et al. (2002)	Threshold; Wavelet reconstruction	Wavelet coefficients based on Shannon entropy	*k-means* clustering
Wang et al. (2006)	NEO + threshold	PCA	Subtractive; *k-means* clustering; template matching
Vargas-Irwin and Donoghue (2007)	Threshold	PCA	Density grid contour clustering; template matching
Fee et al. (1996)	Threshold	Waveform alignment based on multi-electrode waveform pair	Bisection clustering; iterative fusion of cluster processes
Wood et al. (2004)	Threshold	PCA	Spectral clustering; EM with MoG
Sato et al. (2007)	Peak–peak threshold	PCA	Iterative *k-means* using DBVI; template matching
Kim and Kim (2003)	–	Projection pursuit/neg. entropy maximisation	EM with MoG
Kim and Kim (2000)	NEO + threshold	Spike shape	Artificial neural network (MLP with RBFN)
Shoham et al. (2003)	Threshold	PCA	EM with *t*-distributions
Biffi et al. (2008)	Adaptive noise filtering; pos. + neg. threshold detection	PCA	Hierarchical clustering
Zhang et al. (2004)	Threshold	PCA	Subtractive clustering; template matching
Horton et al. (2007)	Threshold	PCA + spike shape curve indices	Kohonen network
Oweiss and Anderson (2002)	Threshold	Wavelet packet decomposition; best basis evaluated by SVD	–
Quiroga et al. (2004)	Threshold	Wavelet packet coefficients (Lilliefors test)	Superparamagnetic clustering
Choi et al. (2006)	MTEO	PCA	Fuzzy c-means clustering
Vogelstein et al. (2004)	SVM	Spike shapes	SVM
Chen et al. (2011)	NEO + threshold	Wavelet coefficients evaluated by PCA	Watershed algorithm
Takegawa et al. (2010)	Threshold	Wavelet coefficients evaluated by distribution	Variational Bayes clustering using *t*-distributions

2007). However, since the result depends on prior template extraction methods, which usually include the already-mentioned clustering techniques, inaccuracies cannot always be compensated.

In conclusion, there still seems to be no optimal method that is generally capable of sorting neural spike patterns. One reason for this might be the lack of fundamental test datasets containing a principal spectrum of theoretically possible spike shapes that could be used to evaluate the different classification algorithms. As this problem also prevents a thorough evaluation of the suitability of different spike features, it is generally difficult to evaluate the feasibility of specific types of features such as principal components or Wavelet coefficients. Although certain studies have shown that Wavelet-based feature extraction potentially outperforms the PCA, this fact cannot be generalised to all possible datasets (Pavlov et al., 2007). Therefore, an a priori exclusion of PCA features can limit the ability to discriminate between certain spike forms. In fact, this is also true for other features that might be inferior in most cases but not in general. Hence, it might not be useful to focus on a specific feature extraction technique, as other features might be more suitable on specific occasions. Therefore, in contrast to most methods, the algorithm presented in this paper regards various possible features, such as principal components and different Wavelet packet coefficients, as well as geometric features. As such an approach requires a unique feature reduction step in order to determine the features most suitable for the particular spikes of the signal, a newly developed feature evaluation step is proposed in this paper. By analysing the probability distribution of the different feature coefficients, the candidates with the most distinctive multimodal character can be found. Resembling the different spike shape characteristics, this method allows the derivation of spike sorting feature sets that are customised for each individual set of neuronal data.

3. Method

After the short overview of spike sorting algorithms given in the previous chapter, the fundamental theory of the method presented in this paper is described in the following.

3.1. Feature extraction

The implementation of a generalised feature evaluation step in the spike sorting process does not only provide the opportunity to use a mixture of PCA and Wavelet features for the classification step, but also allows the inclusion of other features that are, for example, based on the shape of the measured spikes themselves. Certain characteristics of the spike, e.g. its negative or positive amplitude, as well as various gradients or its signal energy can be used as additional candidates. On the one hand, such geometry-based features are usually vulnerable to noise signals and voltage offsets. On the other hand, they can be very potent in particular situations, in which such a feature can specifically highlight a difference between two spike shapes. Furthermore, these features can be quickly and easily calculated and represent no imminent threat to the algorithm's computational complexity (see Table 2).

3.1.1. Geometric features

The calculation of the positive and negative amplitude is basically self-explanatory. The left and right spike angles represent the left and the right gradient of the characteristic spike minimum to the point in the signal, at which it crosses the margin of 50% of that value, as shown in Fig. 2. The choice of this particular margin can be explained by low liability to the noise components of the signal. The resulting value can easily be transformed into an angular measure, using basic trigonometric functions. In addition, the spike duration can be approximated as the distance between the

Table 2
Overview of neuronal signal features.

Feature	Advantages	Disadvantages
Negative amplitude	Easy to interpret	Vulnerable to signal offsets
Positive amplitude	Stresses specific shape characteristics	Only suitable in particular cases; vulnerable to signal offset
Left/right spike angle	Stresses specific shape characteristics	Only suitable in particular cases; vulnerable to noise distortions
Neg./pos. signal energy	Robust features in terms of noise distortions or low sample rates	Naturally correlates with amplitude and angle features; vulnerable to signal offsets
Core spike duration	Stresses specific shape characteristics	Only suitable in particular cases; vulnerable to noise distortions
NEO coefficient	Higher resolution than negative amplitude in particular cases	Naturally correlates with negative amplitude
Principal components	Usually accurate description of datasets with a set of uncorrelated parameters	Possible inaccuracies if more than two spike shapes are present in the dataset
Distribution/Shannon Wavelet coefficients	Potent Wavelet scale features with no significant correlation	High computational complexity compared to other methods; multi-resolution analysis limited by sample rate

intersection points of both gradients with the 0 V level. The positive and negative signal energy of a continuous-time signal $s(t)$ can be approximated based on the following equation (Ohm and Lüke, 2010):

$$E_s = \int_{-\infty}^{\infty} s^2(t)dt \quad (1)$$

Likewise, the signal energy can also be calculated for discrete-time signals by summing the squared discrete signal values. In this case, the positive and negative energy components of the spike are calculated in particular to separate monopolar from bipolar spike shapes more accurately.

3.1.2. NEO coefficients

The value of the NEO operator $\Psi(x[n])$ is calculated for the characteristic spike minimum value with the equation below (Choi et al., 2006):

$$\Psi(x[n]) = x^2[n] - x[n-1] \times x[n+1] \quad (2)$$

The resulting parameter $\Psi(x[n])$ gives an estimate of the energy content of the signal at the discrete time step n of the signal $x(n)$.

3.1.3. Principal components

The first four principal components are derived by the standard principal component analysis (PCA) algorithm based on the eigenvectors and their corresponding eigenvalues of the covariance

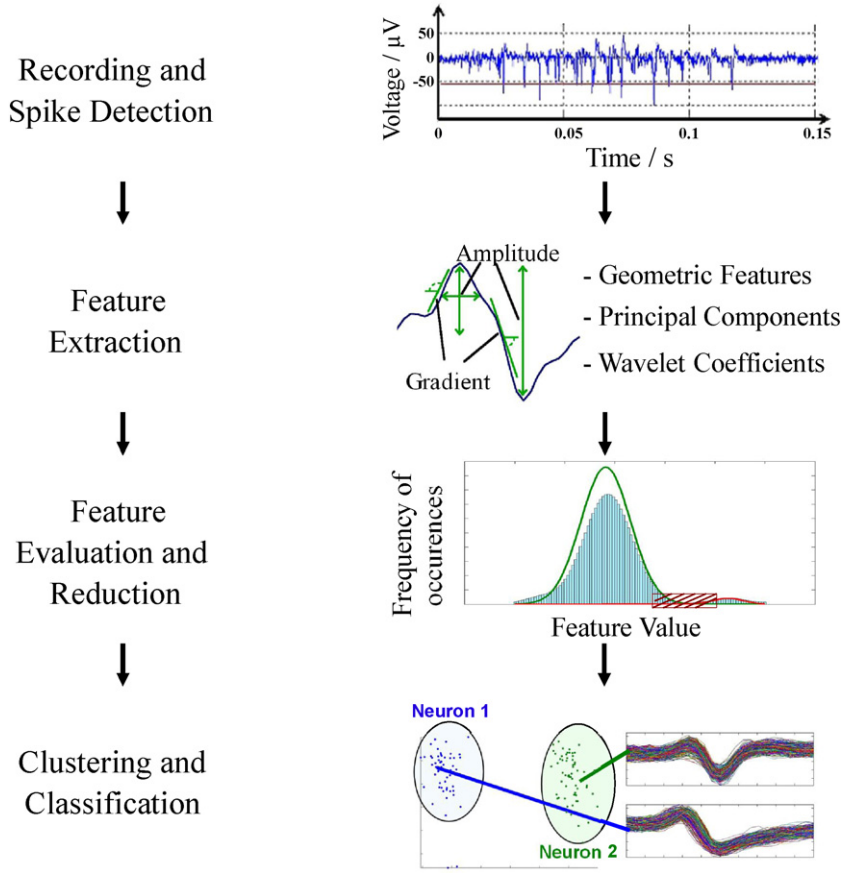

Fig. 2. Overview of the described spike sorting method.

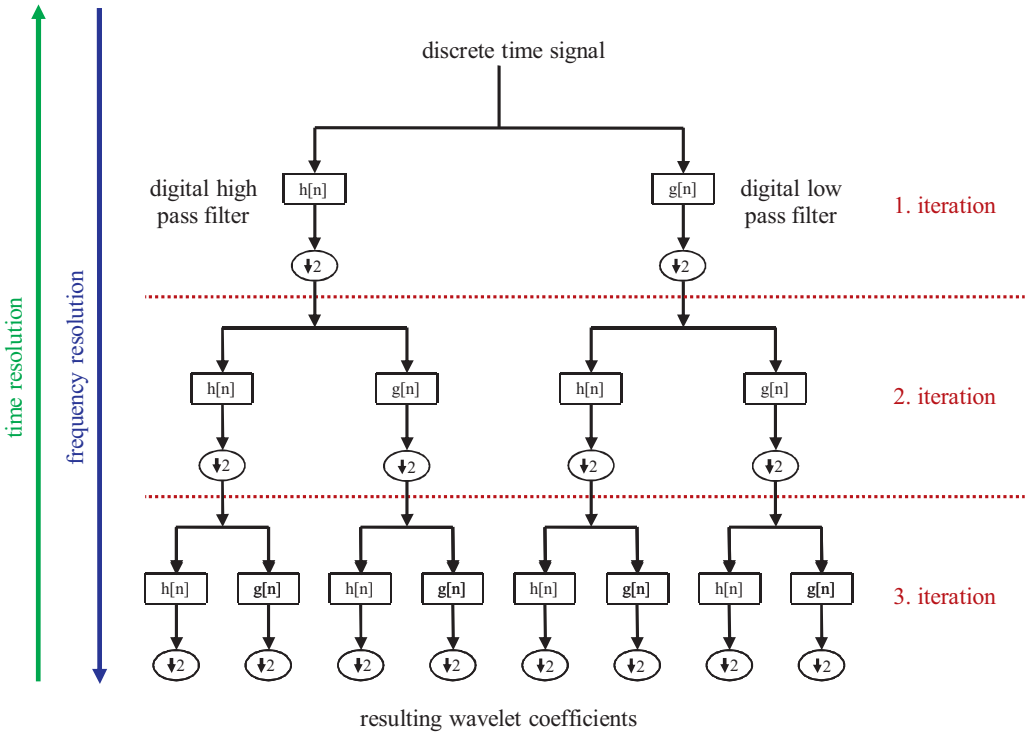

Fig. 3. Schematic of the WPD multi-resolution analysis.

matrix (Joliffe, 2002). The latter is computed with all the voltage values representing the shape of each spike, for all spike events found in the previous spike detection step.

3.1.4. Wavelet coefficients

Two different types of Wavelet coefficients are calculated using the Wavelet packet decomposition (WPD), which is an extension of the standard discrete multi-resolution Wavelet analysis. The Wavelet transformation of a continuous-time signal can be written as such (Stark, 2005):

$$L_\Psi f(a,t) = \frac{1}{\sqrt{(|a|)}} \int_{-\infty}^{\infty} \Psi\left(\frac{u-t}{a}\right) f(u)\ du \tag{3}$$

where the function $\Psi_{a,t}(u)$ denotes the resulting Wavelet based on a specific mother Wavelet and modified by the two independent variables a and u. The latter is an additional time variable describing the temporal shift of the Wavelet with respect to the actual signal, while the actual frequency or scale decomposition is varied by the parameter a. In other words, different scaling values of a generate different daughter Wavelets, a modification of the mother Wavelet, which highlights specific frequency areas in the decomposed signal. For discrete-time signals, an iterative Wavelet decomposition process, also called multi-resolution analysis, is usually described as a filtering process that breaks up the subjacent time signal at a low-pass and a band-pass scale with each iteration. Hence, the resulting frequency scale resolution increases with every step of the process, whereas the time resolution decreases respectively with each splitting. As the ratio between frequency and time resolution is predefined by the uncertainty principle, the standard discrete Wavelet transform (DWT) multi-resolution analysis only focuses on the low-pass component in subsequent iterations, since an accurate frequency determination is especially crucial in this particular range. In contrast, the WPD continues to decompose both the high- and low-pass component with each step of the analysis (see Fig. 3).

This allows a more accurate signal analysis at the expense of additional computational complexity. The result is usually referred to as the Wavelet packet tree (see Fig. 3), with a different set of Wavelet coefficients, called nodes, for each Wavelet filter. Each of these coefficients describes the magnitude of a certain frequency range in a specific time interval, which results in a considerable amount of redundant information with every additional iteration. As a consequence, the most crucial step with respect to the spike sorting task is probably the derivation of the Wavelet scale coefficients that describe the differences of the spike shapes detected in the actual time signal.

The Shannon information criteria can be used to determine the amount of information explained by each node of the Wavelet packet tree (Hulata et al., 2002). Based on the resulting values calculated for every decomposed spike, it is possible to evaluate the divergence of explained information for all nodes throughout all spike events. The most suitable node can be analysed based on the distribution of the values of the Shannon information criteria across every spike. Under the assumption that two different spike shapes produce a multimodal distribution at certain nodes, a determination of these can provide useful feature type for the spike sorting process.

To obtain a second type of Wavelet-based features, the same process can be implemented for the resulting Wavelet packet coefficients themselves. Again, the goal is to find a coefficient that shows a multimodal distribution considering its value across all detected spikes. Therefore, the fundamental extraction algorithm is identical and only the input variables are actually changed.

In the proposed algorithm, three Wavelet coefficients for both types with the most promising probability distribution were chosen as spike sorting features. In other words, the best three Wavelet coefficients calculated with the Shannon information criteria as well as the best three Wavelet coefficients with respect to their natural distribution were used. As only the resulting distribution and not the calculated values themselves were of interest, the Haar Wavelet (Stark, 2005) was chosen as the mother Wavelet for

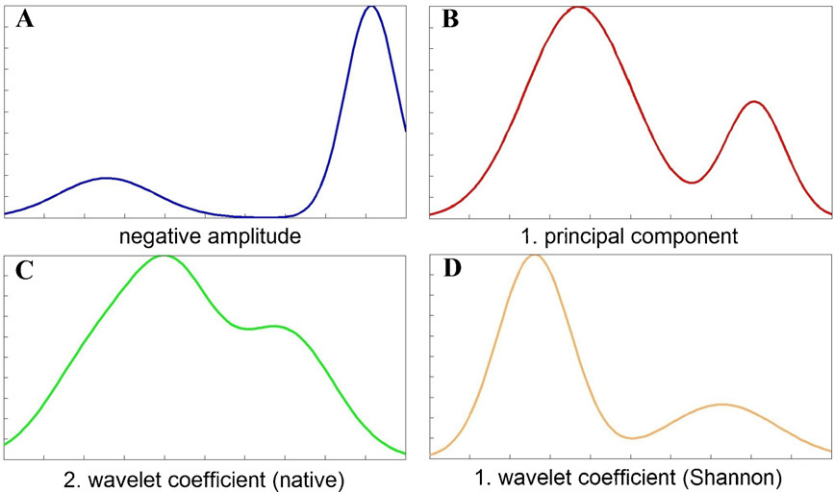

Fig. 4. Example of different feature distributions extracted from a neuronal dataset. The "negative amplitude" and the "first principle component" in A and B, respectively, seem to be suitable, whereas the second native Wavelet coefficient in C only offers a limited perspective. The first Shannon Wavelet coefficient in D may also be quite suitable, but its distribution is less distinctive compared to that in B.

the multi-resolution analysis, since it provides the fastest computing time without significantly changing the outcome compared to other mother Wavelets. To avoid a highly redundant feature set, the correlation between the candidates was also taken into account. Even a promising Wavelet coefficient was discarded if its correlation value with respect to the superior coefficients already chosen crossed a certain threshold value.

In conclusion, the distribution approach analyses the decomposition result in further detail; however, it also requires a considerable amount of additional computation time compared to the Shannon entropy-based method. Nevertheless, as each approach can identify distinct spike characteristics, it is beneficial to extract both types of Wavelet features for further evaluation.

3.2. Feature evaluation and reduction

With every spike sorting feature calculated, the key is to find the set that is most suitable for the task at hand. Therefore, it is important to keep evaluating the feature's distributions with respect to their separability. In the following section, the crucial part of the presented algorithm is described, which is used to evaluate and compare the extracted features. For the sake of clarity, this is the same algorithm that was applied to identify the most suitable Wavelet coefficients for both Wavelet feature types.

To further specify the actual goal of the algorithm, it is helpful to look at certain distribution functions that can be found in this context (see Fig. 4).

Looking at Fig. 4, it is quite obvious that the two features in Fig. 4A and B seem to be promising examples with a clearly identifiable multimodal character, possibly allowing the separation of two spike shapes. Thus, the desired feature distribution should not only show at least two distinct maxima, but also ought to be clearly separated from each other. Therefore, as both criteria should be ideally described in a single value, this inevitably leads to some blurriness when evaluating the various feature candidates. As a consequence, it is crucial that both criteria are rated as accurately as possible in order to minimise the resulting uncertainty. Hence, the expectation maximisation (EM) method was chosen for this purpose, as it offers suitable parameters for assessment. An EM algorithm using Gaussian basis functions was selected, assuming that the sum of the noise components, usually present in every measurement data, leads to a Gaussian distortion of generally stable spike shapes. The EM algorithm is used to approximate the calculated distribution of each feature with a so-called mixture of Gaussians (MoGs) that can be mathematically described with the following equation (Polanski and Kimmel, 2007):

$$f^{\mathrm{mix}}(x, \alpha_1, \ldots, \alpha_k, p_1, \ldots, p_k) = \sum_{k=1}^{K} \alpha_k f_k(x, p_k) \tag{4}$$

where α_k specifies the weight of each function within the mixture model and p_k denotes its actual parameters. In turn, every Gaussian component is specified with its characteristic formula:

$$f_k(x, p_k) = f_k(x, \mu_k, \sigma_k) = \frac{1}{\sigma\sqrt{(2n)}} \exp\left(\frac{(x-\mu)^2}{2\sigma_k^2}\right) \tag{5}$$

Therefore, the EM algorithm needs to scale the values μ_k, σ_k and α_k for each mixture component. To find a suitable approximation, it iterates between two distinctive steps, the expectation (E-step) and the maximisation (M-step). At the start of the process, either a random or an a priori value is presumed for each parameter. On this basis, the difference $Q(p, p^{\mathrm{old}})$ between the actual distribution and the current approximation is calculated in the E-step, using the log-likelihood function (Polanski and Kimmel, 2007):

$$Q(p, p^{\mathrm{old}}) = \sum_{n=1}^{N}\sum_{k=1}^{K} p(k|x_n, p^{\mathrm{old}}) \ln \alpha_k + \sum_{n=1}^{N}\sum_{k=1}^{K} p(k|x_n, p^{\mathrm{old}}) \ln f_k(x_n, p_k) \tag{6}$$

The parameter N equals the number of data points of the feature distribution, while K still denotes the number of Gaussians in the mixture. In the subsequent M-step, a new set of parameters is determined to improve the parity between approximation and feature distribution. In this case, the parameters p_k, μ_k^{new}, σ_k^{new} and α_k^{new} can be calculated with the following set of equations (Polanski and Kimmel, 2007):

$$\mu_k^{\mathrm{new}} = \frac{\sum_{n=1}^{N} x_n \times p(k|x_n, p^{\mathrm{old}})}{\sum_{n=1}^{N} p(k|x_n, p^{\mathrm{old}})} \tag{7}$$

$$(\sigma_k^{\mathrm{new}})^2 = \frac{\sum_{n=1}^{N} (x_n - \mu_k^{\mathrm{new}})^2 \times p(k|x_n, p^{\mathrm{old}})}{\sum_{n=1}^{N} p(k|x_n, p^{\mathrm{old}})} \tag{8}$$

$$\alpha_k^{\text{new}} = \frac{\sum_{n=1}^{N}(k|x_n, p^{\text{old}})}{N} \quad (9)$$

These new parameters can be evaluated and refined with another iteration of the E-step and M-step, respectively, either until $Q(p, p^{\text{old}})$ cannot be improved any further or until a certain threshold criterion is met.

To facilitate the approximation process, each native feature distribution, derived with its histogram, is smoothed in order to limit the effects of outlying data points. Furthermore, the number and corresponding positions of existing maxima are determined by simple curve sketching and serve as initial values for the EM process.

Once the final approximation result is acquired, the obtained parameters provide a suitable basis for evaluation. Whereas the distance between each Gaussian component in the mixture is expressed by μ_k^{new}, α_k^{new} models the distinction of the individual functions, while σ_k^{new} can be used to determine the overlapping of the identified Gaussians. As it is hard to determine any hierarchy among these parameters, their values have to be transformed into an overall rating for the examined features. For this purpose, the following equation has been specifically designed to provide a solution to the resulting problem:

$$v(k) = \frac{\sum_{k\neq 1}^{K} Cov(i,k)}{(\mu(\max) - \mu(k)) \times \alpha(k)} \quad (10)$$

The value $v(k)$ rates the distinctiveness of an individual Gaussian function, k, present in the mixture compared to the Gaussian surrounding its global maximum, denoted by $\mu(\max)$. Only the covariance measure puts every mixture component into account, to accurately express the actual overlap. As described in Section 3.3, the presented spike sorting algorithm is specifically designed to separate two specific clusters. Therefore, the features showing a bimodal characteristic are of particular interest. As a consequence, in the first step $v(k)$ is calculated individually for every Gaussian component of each mixture. Afterwards, the minimum value for $v(k)$ over all components of the mixture is determined and serves in as an overall rating for the corresponding feature. In addition, features that appear to have only a unimodal distribution are also evaluated by the variance they explain, but are treated as secondary candidates.

It is this rating that allows the derivation of a unique feature set for each individual dataset. The particular candidates that minimise $v(k)$ are selected, although again with the correlation as an additional criterion. In this algorithm, the maximum subset size was adjusted to six, simply to limit the computational complexity of the subsequent clustering process. However, it is possible that this number is not reached, as the correlation criteria can further limit the size of the determined subset.

3.3. Clustering

As the final step in the spike sorting process, the resulting feature set has to be classified into distinct clusters that contain the particular spikes of an individual neuron. For this purpose, the derived subset is first used to span a multidimensional feature space. In order to identify the clusters involved, the EM algorithm is used once again. On the one hand, this clustering method has the advantage of providing a soft classification result, which allows the exclusion of outliers, unlike, for example, the *k-means* algorithm (Clarke et al., 2009). On the other hand, as a plain clustering algorithm, it does not require any training process in advance, which is especially advantageous in this case.

Similarly to the feature evaluation step described in the previous chapter, the EM algorithm approximates the data distribution of a given space, using Gaussian basis functions. Consequently, each data point, resembling a specific spike event, is sorted into the resulting mixture components based on the probability associated with each Gaussian. As mentioned before, the algorithm is designed to specifically separate the data into two Gaussian clusters. First of all, this eliminates the problematic task of determining the number of clusters, i.e. the number of spiking cells. Secondly, this gives the opportunity to derive feature sets that can resemble the difference in shape of the remaining spike signals more accurately, thereby enhancing the separability. The described algorithm is generally able to cluster the data into more than just two classes. Nevertheless, in the proposed algorithm, an iterative approach is favoured, as it gives the opportunity to separate one specific class from the rest of the signal in each iteration. Thus, the derivation of suitable features becomes significantly easier, improving the subsequent clustering result. As a final consequence this approach basically minimises the chance of oversorting, which means the separation of the spikes of one individual cell into multiple clusters, since the feature evaluation primarily credits the distinctiveness of the Gaussians in the mixture of a feature rather than the number of Gaussians in it. Though MoG's with more than two Gaussian components are not excluded in general, the covariance criteria of Eq. (10) ensures that such features are picked, only if these components can be clearly separated.

4. Results and discussion

The algorithm described in the previous chapter was implemented in a self-made Matlab©-based software. To test the feasibility of the developed algorithm, both simulated data and recorded data derived from 3D neuronal cell cultures, so-called spheroids (Layer and Willbold, 1993; Layer et al., 2002), were used.

4.1. Results with simulated data

Simulated datasets were primarily applied to validate the results of the described spike sorting algorithm. Such simulated data samples have the advantage of being labelled and better suited for the testing of a general algorithm. Hence, simulated data published for such purposes by the University of Leicester was used (cf. Quiroga et al., 2004). It offered various examples of neuronal data, simulated at a sample rate of 24 kHz. The different sets also varied in their signal-to-noise ratio (SNR), allowing an evaluation of the sorting results as a function of SNR. As an exemplary dataset, the file *c_difficult2_noise01* with a SNR of 10 was applied (see Fig. 5).

The dataset contained three basic spike shapes that were randomly distorted by Gaussian noise components. As a preliminary step, the spike events were detected at a simple voltage threshold that was calculated based on the standard deviation of the noise contained in the signal (Chiappalone et al., 2005). To exclude any unwanted noise events that were detected, a first sorting iteration was performed.

Next, the actual spike sorting task was met with a second iteration of the spike sorting algorithm. Various spike features were calculated for each spike event, based on a 1 ms window (24 data points) around the detected time-stamp at its voltage minimum. In the first attempt, the data were clustered via the EM algorithm, applying Wavelet-based features exclusively and in another sorting attempt, principal components only (see Fig. 6). In order to improve clarity, the clustering result was projected only on the first two dimensions of the multidimensional feature space. To exclude outlying data points usually originating from highly distorted or overlapping spikes, a confidence probability interval of 5% was used. In other words, data points belonging to a certain cluster with a probability of less than 5% were separated into a special cluster. Neither combination, although mainly used in common

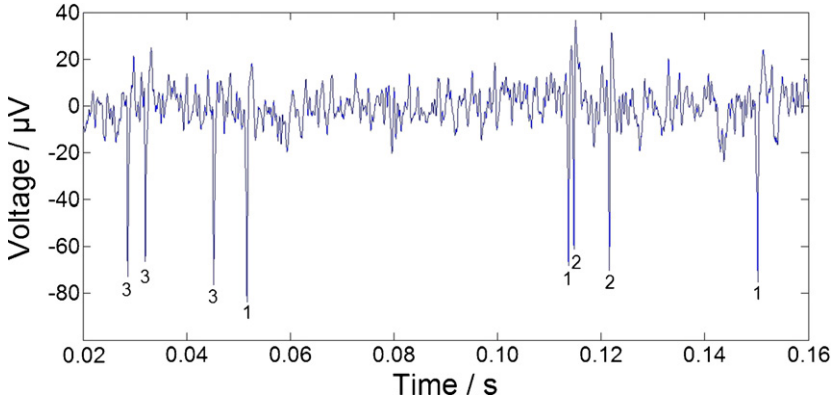

Fig. 5. 150 ms section of the simulated data sample of data from the University of Leicester. The signal, sampled at a rate of 24 kHz, contains three basic spike shapes with an SNR value of 10. In order to process the data with the analysis framework, the normalised sample was multiplied with an offset value of 70 µV. Furthermore, the signal was inverted, as the spike detection algorithm of our Matlab© interface generally expects neuronal spikes with negative amplitudes. The different spike shapes are marked with their respective cluster number.

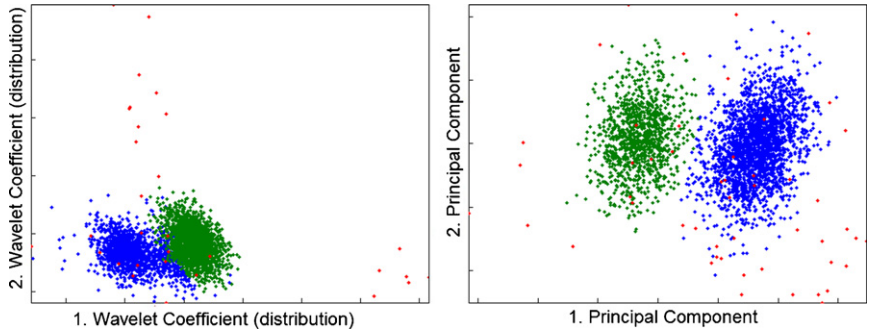

Fig. 6. Clustering result of the dataset *c_difficult2_noise01* using the EM algorithm only with Wavelet-based features, in detail the three Wavelet packet coefficients with the most suitable probability distribution (left) and only with the first three principal components, describing 90% of the data's variance (right). For improved clarity, the plots only show a projection of the multidimensional feature space onto the first two features. Neither combination correctly separated all three spike shapes, as only two distinct clusters could be determined. Outlying data points were separated into a particular cluster using a confidence probability interval of 5%.

algorithms, could separate all three spike shapes in the particular feature space correctly.

Hence, the subsequent spike sorting result was not satisfying either. In the next step, the novel automated feature evaluation algorithm was used to find a suitable mixture of spike shape features. The determined set of features was then fed into the subsequent clustering step. Fig. 7 shows the result of the EM algorithm

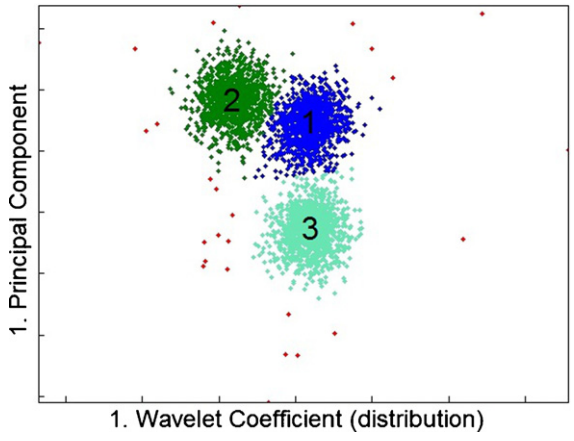

Fig. 7. Clustering result of the dataset *c_difficult2_noise01* using the (1) Wavelet coefficient (distribution) and the (1) principal component. The sorting algorithm could separate the three distinct clusters, while outlying data points were separated into a particular cluster using a confidence probability interval of 5%.

in the two-dimensional feature space spanned by the two best features, namely the first principal component and the first Wavelet coefficient evaluated from its distribution.

In the feature space seen in Fig. 7, three clusters instead of two were identified. Hence, the feature combination found by the algorithm clearly described the particular dataset more accurately than the sets of the two previous approaches.

Therefore, the mixture of different types of features provides a better clustering result compared to the common attempts with one particular type only used in most of the algorithms already established. To look at the results in further detail, the sorting result was evaluated for each spike by comparing the calculated classification result and the original label (see Table 3).

If the events of overlapping spikes are excluded, the spike sorting algorithm almost yields a perfect result, with only nine falsely clustered events. This number, however, is significantly decreased, once overlapping events are taken into account. In order to examine the algorithm's results in more detail, the errors made between missing and incorrectly assigned spikes in a certain cluster are summarised in Table 4.

Most spikes classified in one of the three clusters were sorted correctly, even when considering overlapping events. This phenomenon can be explained by two separate errors. First, spikes that follow too closely after one another were detected not as two different but one single event. Hence, one of the two contained spikes was basically omitted and therefore, lost before the sorting step. Second, if both spikes were detected separately, but distorted each other's shape too drastically, they were usually discarded into a

Table 3
Comparison of original and calculated spike sorting results, using the dataset *c_difficult2_noise01* with a SNR of 10.

Classes	No. of original spikes (with overlapping spikes)	No. of correctly sorted spikes (with overlapping spikes)	% of correctly sorted spikes (with overlapping spikes)
Overall	2742 (3462)	2733 (3351)	99.67 (96.79)
Cluster 1	957 (1187)	953 (1146)	99.58 (96.55)
Cluster 2	898 (1136)	898 (1113)	100 (97.98)
Cluster 3	887 (1139)	882 (1092)	99.44 (95.87)

Table 4
Classification of the resulting clustering errors of the algorithm, using the dataset *c_difficult2_noise01* with a SNR of 10.

Classes	No. of correctly sorted spikes (with overlapping spikes)	No. of missed spikes (with overlapping spikes)	No. of false positives (with overlapping spikes)
Overall	2733 (3351)	9 (111)	9 (14)
Cluster 1	953 (1146)	4 (41)	5 (5)
Cluster 2	897 (1112)	0 (23)	1 (1)
Cluster 3	883 (1093)	5 (47)	3 (8)

special remnant cluster (see red cluster in Fig. 7). In other words, only overlapping spikes that still showed a certain amount of its distinctive shape could actually be processed correctly.

One way of facing the challenge of overlapping spikes is by implementing an additional template matching step, which refines the discarded spike events. By finding a combination of the discovered spike shapes in the spike sorting step that matches the shape of an event inside the remnant cluster, the spikes involved can be identified (cf. Zhang et al., 2004).

In order to evaluate the influence of different noise levels, the algorithm was also tested with another dataset with a SNR of 6.67. The used set *c_difficult2_noise015* basically consists of the same three spike shapes as the data above, yet the distribution of the different spikes is changed slightly. Due to the increased noise distortion it is more difficult to find suitable spike features that can discriminate all three shapes in just one feature extraction step. Hence, using the first two Wavelet coefficients (distribution) and the first two principal components, the algorithm could only separate one of the cell signals from the other, but not all signal shapes in the initial process. In this case the advantage of the iterative structure of the proposed algorithm comes into effect. As it is much easier to find features that specifically describe the differences of the two remaining spike shapes, the sorting result is greatly improved once the first cell signal is excluded from the dataset. Using the adjusted first and second Wavelet coefficients (distribution) as well as the adapted first principal component the two remaining cell signals can be separated from each other. In a final iteration the remaining spike shape can be excluded from the obligatory remnant cluster. The result of this process is summarised in Tables 5 and 6, which are structured similar to Tables 3 and 4 of the first dataset.

As expected the accuracy of the spike sorting process deteriorates with increasing signal-to-noise ratios. In this case both the result discarding overlapping spikes as well as result that includes these events are effected by about the same margin. Even though the increased signal-to-noise ratio poses an additional challenge, the majority of the spikes contained in the data were successfully sorted in the correct clusters. Thus the novel feature extraction and evaluation steps of the described algorithm show significant advantages compared to the methods common in most established spike sorting algorithms, especially when used in an iterative process.

4.2. Results with spheroid data

To further assess the presented spike sorting algorithm, data obtained from chick embryonic neurons coupled to microelectrode arrays were used.

For this purpose chick neuroepithelial tissue (stages 28 and 29, Hamburger and Hamilton (1951)) was chopped and enzymatically dissociated with Trypsin/EDTA (all chemicals: CCPro, Oberdorla, Germany, unless stated otherwise), similarly as described for cardiac tissue in Egert and Meyer (2005). Approximately 2 million cells were transferred to 35 mm Petri dishes containing 2 ml of cell culture medium (DMEM with 10% FCS, 2% CS (Sigma, Munich, Germany), 0.5 mM glutamine, 50 U/ml penicillin, and 50 μg/ml streptomycin). The cells were re-aggregated into three-dimensional spherical in vitro networks, so called spheroids, by

Table 5
Comparison of original and calculated spike sorting results, using the dataset *c_difficult2_noise015* with an SNR of 6.67.

Classes	No. of original spikes (with overlapped spikes)	No. of correctly sorted spikes (with overlapped spikes)	% of correctly sorted spikes (with overlapped spikes)
Overall	2631 (3440)	2577 (3243)	97.95 (94.27)
Cluster 1	858 (1142)	839 (1065)	97.78 (93.28)
Cluster 2	851 (1113)	824 (1040)	96.83 (93.44)
Cluster 3	922 (1185)	914 (1138)	99.13 (96.03)

Table 6
Classification of the resulting clustering errors of the algorithm, using the dataset *c_difficult2_noise015* with an SNR of 6.67.

Classes	No. of correctly sorted spikes (with overlapped spikes)	No. of missed spikes (with overlapped spikes)	No. of false positives (with overlapped spikes)
Overall	2577 (3243)	54 (197)	53 (92)
Cluster 1	858 (1065)	19 (77)	34 (49)
Cluster 2	851 (1040)	27 (73)	7 (26)
Cluster 3	922 (1138)	8 (47)	12 (17)

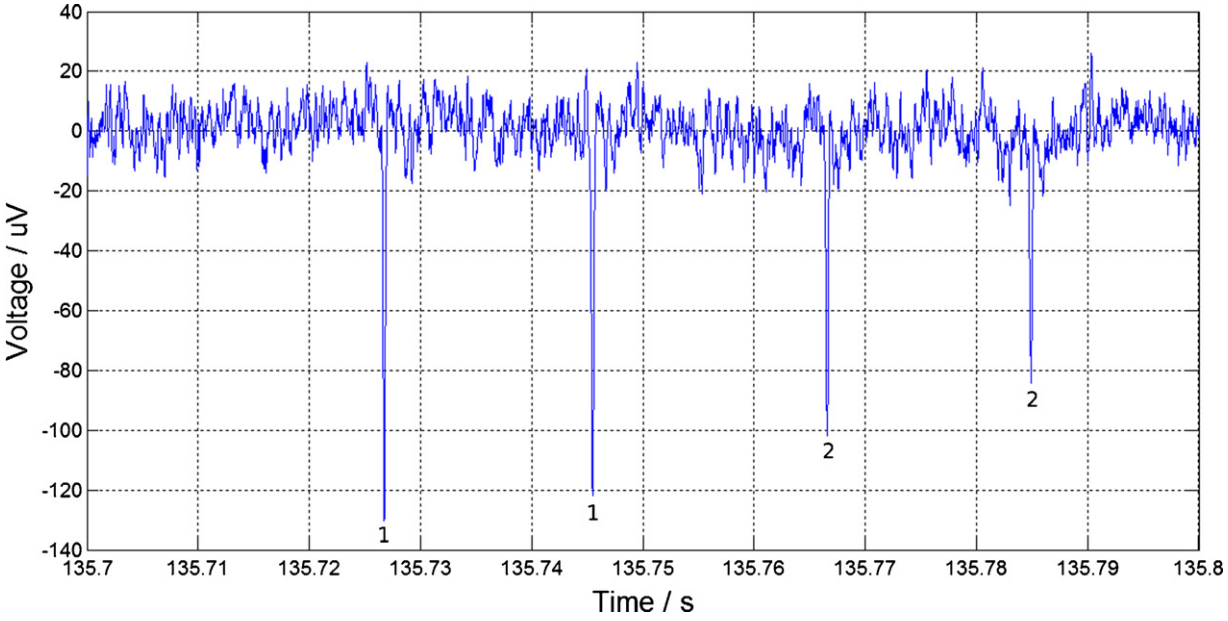

Fig. 8. 100 ms section of the recorded spheroid data sample, recorded with 50 kHz. The spikes were labelled according to the clustering result of the subsequent classification (cf. Fig. 9).

placing the Petri dishes on a gyratory shaker (72 rpm) within an incubator (37 °C, 5% CO_2) (Daus et al., 2011).

The resulting spheroids were then plated on microelectrode arrays (MEA; Multichannel Systems, Reutlingen, Germany) for extracellular recording. The MEA chips consisted of 60 substrate-embedded titanium nitride electrodes (30 μm in diameter) arranged in an 8×8 matrix. Extracellular field potentials, so-called spikes, were recorded (25–50 kHz sampling rate) and saved for offline analysis. The timestamps of the spikes were determined by a threshold separating neuronal signals from noise (Chiappalone et al., 2005). These data pose an additional difficulty, as multiple neurons contribute to the electrode signal. However, most of these neurons had an insufficient coupling with the electrode, which significantly hampered the ability to separate the particular spike shapes of the emitting neurons (see Fig. 8).

The spike detection process for this type of data was as described above. However, due to the signal's complexity, a supplementary sorting step was necessary to exclude any shapes originating from distant neurons that could not be satisfyingly processed and only acted as additional noisy artefacts.

Similar to the evaluation process using the simulated data, the spikes of the spheroid signal were sorted using either Wavelet-based features, principal components or the feature mixture derived by our novel approach. All methods could identify two different spike shapes in the spheroid signal, which means that the recorded spheroid signal contained at least the signals of two neurons, with a tight coupling to the electrode (cf. Fig. 9). Yet the different feature extraction approaches show a varying ability to discriminate between the two shapes. The resulting clusters of the Wavelet-based approach showed a significant overlap, unlike the other two methods. The result using principal components however was quite similar to the clustering of our proposed mixture approach, only with slight differences at the border between the two identified clusters. Even though the result using the feature mixture of the proposed algorithm might be considered marginally more accurate, such improvement would be quite difficult to assess, due to the lack of labelling for the recorded spheroid data.

In general, even though both Wavelet and principal component based feature extraction techniques are capable of producing acceptable spike sorting results, they usually fail to achieve an optimal discrimination between different cell signals, simply due to their lack of variability. Whereas our algorithm includes the strength of principal components without neglecting the potency of other features, the methods using only a single feature type suffer from their respective weaknesses. Hence, it is most feasible to include both feature types in order to preserve their strengths and to compensate their weaknesses respectively.

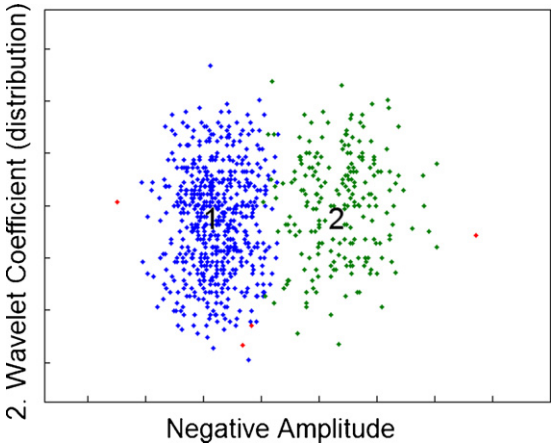

Fig. 9. Scatterplot of the spheroid data in the feature space spanned by the negative amplitude and the (2) Wavelet coefficient (distribution). Again the scatterplot shows a projection of the clustering results onto the two dimensional feature space of first and second feature. The data can be sorted into two spike shape clusters using the (2) principal component as additional feature. The data points in red again highlight the remnant cluster containing outliers in the spheroid data. (For interpretation of the references to color in this figure legend, the reader is referred to the web version of the article.)

5. Conclusion and outlook

In summary, the described algorithm yields accurate results for simulated and recorded neuronal datasets. The concept of evaluating a broad set of extracted features to find a suitable subset that describes a particular dataset most accurately seems to have certain advantages. Instead of relying on the potency of a single

feature type, the different capabilities of various feature extraction techniques become available for the subsequent sorting stages and therefore, significantly facilitate the clustering task. Therefore, this enables even a comparably simple EM classification method to produce a precise clustering result.

Based on this feature evaluation technique, it is also possible to identify the features that explicitly discriminate between two different spike shapes, which is advantageous in neural recordings that include more than just two signal shapes. This ability is used by the presented algorithm, given that an iterative subtraction process of particular spike shapes from the rest of the signal can be performed if necessary. This allows the identification of a new feature subset most suitable for the remaining spikes in the dataset after excluding a certain shape.

The only issue that could be identified is the lack of an adequate handling of overlapping spike events. Nevertheless, this can be fixed quite easily with an additional template matching step based on the algorithm's clustering result.

There might still be some room for useful adaptations. One possible approach, for example, is the use of *t*-distributions instead of Gaussians as a basis function (Shoham et al., 2003). With an additional adjustment parameter, the degrees of freedom (DOF), these functions might be more robust to any non-Gaussian noise distortions. However, as a drawback, this additional parameter could also result in a significantly higher computational complexity.

On the other hand, the EM algorithm itself could be substituted with the Variational Bayes (VB) algorithm (Takegawa et al., 2010). Being a more general approach than EM, it offers the same advantages, but also disadvantages, as the switch from Gaussian to *t*-distributions.

Another issue necessary to address is the computational complexity of the algorithm itself. The time required to approximate the distribution of a certain feature significantly depended on the particular distribution characteristics. Therefore, it is hard to generate a generalised statement regarding the processing time needed by the algorithm. However, the current version of the algorithm has to be modified in order to function in an online signal analysis process. For this purpose, it is possible to compute explicit operations in parallel, using multiple CPU or GPU cores (cf. Chen et al., 2011). Thus, the approximation of different features via the EM algorithm can be calculated simultaneously, effectively speeding up the spike sorting algorithm altogether.

Although there might be some possible adaptations of the algorithm, its general feasibility and advantages compared to most common spike sorting algorithms are quite obvious. The reason for this is the improved feature extraction approach that enables an adaptive determination of suitable spike sorting features. This allows the inclusion of a variety of different feature types, which increases the chance of identifying particular key differences between a set of unique spike shapes.

In conclusion, the disadvantage of only being able to use a limited subset of feature types that most established spike sorting methods face can be overcome with the novel approaches presented in this paper. Hence, it is also possible to enhance already existing algorithms with these ideas, improving their clustering or classification significantly.

Acknowledgement

This work was supported by the BMBF AN2208PT-AIF.

References

Biffi E, Ghezzi D, Pedrocchi A, Ferrigno G. Spike detection algorithm improvement, spike waveforms projections with PCA and hierarchical classification. IET Conf Pub 2008(CP540):122–6.
Chen Y, Tsai Y, Chen L. Algorithm and implementation of multi-channel spike sorting using GPU in a home-care surveillance system. ICME IEEE 2011(CFP11):1–6.
Chiappalone M, Novellino A, Vajda I, Vato A, Martinoia S, van Pelt J. Burst detection algorithms for the analysis of spatiotemporal patterns in cortical networks of neurons. Neurocomputing 2005;65:653–62.
Choi JH, Jung HK, Kim T. A new action potential detector using the MTEO and its effects on spike sorting systems at low signal-to-noise ratios. IEEE Trans Biomed Eng 2006;53:738–46.
Clarke B, Fokoué E, Zhang HH. Principles and theory for data mining and machine learning. New York: Springer; 2009. p. 408–11.
Daus AW, Goldhammer M, Layer PG, Thielemann C. Electromagnetic exposure of scaffold-free three-dimensional cell culture systems. Bioelectromagnetics 2011;32:351–9.
Egert U, Meyer T. Heart on chip—extracellular multielectrode recordings from cardiac myocytes in vitro. In: Dhein S, editor. Practical methods in cardiovascular research. Springer: Berlin; 2005. p. 432–53.
Fee MS, Mitra PP, Kleinfeld D. Automatic sorting of multiple unit neuronal signals in the presence of anisotropic and non-Gaussian variability. J Neurosci Methods 1996;69:175–88.
Hamburger V, Hamilton HL. A series of normal stages in the development of the chick embryo. J Morphol 1951;88:49–92.
Horton PM, Nicol AU, Kendrick KM, Feng JF. Spike sorting based upon machine learning algorithms (SOMA). J Neurosci Methods 2007;60:52–68.
Hulata E, Segev R, Ben-Jacob E. A method for spike sorting and detection based on wavelet packets and Shannon's mutual information. J Neurosci Methods 2002;117:1–12.
Joliffe IT. Principal component analysis. 2nd ed. New York: Springer; 2002. p. 1–6.
Kim KH, Kim SJ. Neural spike sorting under nearly 0-dB signal-to-noise ratio using nonlinear energy operator and artificial neural-network classifier. IEEE Trans Biomed Eng 2000;47:1406–11.
Kim KH, Kim SJ. Method for unsupervised classification of multiunit neural signal recording under low signal-to-noise ratio. IEEE Trans Biomed Eng 2003;50:421–31.
Layer PG, Willbold E. Histogenesis of the avian retina in reaggregation culture: from dissociated cells to laminar neuronal networks. Int Rev Cytol 1993;146:1–47.
Layer PG, Robitzki A, Rothermel A, Willbold E. Of layers and spheres: the reaggregate approach in tissue engineering. Trends Neurosci 2002;25(3):131–4.
Ohm JR, Lüke HD. Signalübertragung. 11th ed. Berlin: Springer; 2010. p. 203.
Oweiss KG, Anderson DJ. Spike sorting: a novel shift and amplitude invariant technique. Neurocomputing 2002;44:1133–9.
Pavlov A, Makarov VA, Makarova I, Panetsos F. Sorting of neural spikes: when wavelet based methods outperform principal component analysis. Natural Comput 2007;6(3):269–81.
Polanski A, Kimmel M. Bioinformatics. Berlin: Springer; 2007. p. 37–45.
Quiroga RQ, Nadasdy Z, Ben-Shaul Y. Unsupervised spike detection and sorting with wavelets and superparamagnetic clustering. Neural Comput 2004;16:1661–87.
Sakmann B, Neher E. Single channel recording. 2nd ed. New York: Springer; 2009. p. 4.
Sato T, Suzuki T, Mabuchi K. Fast automatic template matching for spike sorting based on Davies–Bouldin validation indices. Conf Proc IEEE Eng Med Soc 2007:3200–3.
Shoham S, Fellows MR, Normann RA. Robust, automatic spike sorting using mixtures of multivariate *t*-distributions. J Neurosci Methods 2003;127:111–22.
Stark HG. Wavelets and signal processing: an application-based introduction. Berlin: Springer; 2005. p. 21–28.
Takegawa T, Isomura Y, Fukai T. Accurate spike sorting for multi-unit recordings. Eur J Neurosci 2010;31:263–72.
Thomas CA, Springer PA, Loeb GE, Berwald-Netr Y, Okun LM. A miniature microelectrode array to monitor the bioelectric activity of cultured cells. Exp Cell Res 1972;74:61–6.
Vargas-Irwin C, Donoghue JP. Automated spike sorting using density grid contour clustering and subtractive waveform decomposition. J Neurosci Methods 2007:164.
Vogelstein RJ, Murari K, Thaku PH, Diehl C, Chakrabartty S, Cauwenberghs G. Spike sorting with support vector machines. In: IEEE EMBS; 2004. p. 4009–12.
Wang G, Zhou Y, Chen A, Zhang P, Liang PA. A robust method for spike sorting with automatic overlap decomposition. IEEE Trans Biomed Eng 2006;53:1195–8.
Wood F, Fellows M, Donoghue JP, Black MJ. Automatic spike sorting for neural decoding. IEEE Trans Biomed Eng 2004;51:912–8.
Zhang P, Wu J, Zhou Y, Liang P, Yuan J. Spike sorting based on automatic template reconstruction with a partial solution to the overlapping problem. J Neurosci Methods 2004;135:55–65.